Electronic Supplementary Material (ESI) for Chemical Communications.

Supporting Information

Construction of Ni^{3+}-rich nanograss arrays for booting alkaline water oxidation

Ruirui Zhang, Jingce Bi, Junbiao Wu, Zhuopeng Wang, Xia Zhang and Yide Han*

Department of Chemistry, College of Science, Northeastern University, Shenyang, 110819, China

*Corresponding author: Dr. Yide Han, Email: hanyide@mail.neu.edu.cn

Experimental section

Chemicals and reagents

Nickel (II) nitrate hexahydrate ($Ni(NO_3)_2 \cdot 6H_2O$), thioacetamide (TAA), sodium orthovanadate ($Na_3VO_4 \cdot H_2O$), sodium molybdate dihydrate ($Na_2MoO_4 \cdot 2H_2O$), potassium hydroxide (KOH), ethanol and methanol were purchased from Sinopharm Chemical Reagent Co., Ltd. 1,3,5-Benzenetricarboxylic acid (BTC) was purchased from Aladdin. Hydrochloric acid (HCl) and acetone (CH_3COCH_3) were acquired from Tianjin Yongda Chemical Reagents. Nickel foam (NF) was obtained from Changde Liyuan New Material Co., Ltd. All reagents were commercially available and used without further purification.

Preparation of Ni-BTC@NF

In order to remove the surface oxides, NF was cleaned by consecutive sonication in acetone, HCl aqueous solution (3 $mol \cdot L^{-1}$) and water for 10 min, respectively. Afterwards, 0.325 g of $Ni(NO_3)_2 \cdot 6H_2O$ and 0.125 g of BTC were dispersed in 18 mL of methanol and stirred magnetically for 30 min. The obtained mixture was transferred into a 25 mL Teflon-lined stainless-steel autoclave reactor, followed by the addition of a piece of NF (2 × 3 cm^2). After that, the autoclave was maintained at 150 °C for 24 h. After the autoclave cooled down to room temperature, the as-obtained Ni-BTC@NF was taken out and rinsed thoroughly with DI water and ethanol for several times, and then dried in an oven at 60 °C for 12 h.

Preparation of Mo-Ni-BTC@NF

At first, 60 mg of $Na_2MoO_4 \cdot 2H_2O$ was dispersed in 25 mL of the mixed solution containing of 20 mL of distilled water and 5 mL of ethanol under magnetic stirring for 30 min. Then, the pre-prepared Ni-BTC@NF was immersed in the above solution and kept at 85 °C for 10 min. After cooling down to room temperature, Mo-Ni-BTC@NF was taken out and washed with DI water and ethanol successively for three times, and then dried in an oven at 60 °C for 12 h in vacuum.

Preparation of Mo-NiVS@NF

Firstly, Mo-Ni-BTC@NF was immersed in 15 mL aqueous solution containing 50 mg of TAA and 50 mg of $Na_3VO_4 \cdot H_2O$. Then the solution together with Mo-Ni-BTC@NF was transferred into a 25 mL Teflon-lined stainless autoclave and kept at 180 °C for 4 h. The product was rinsed by DI water and ethanol successively for three times. After drying in an oven at 60 °C for 12 h, Mo-NiVS@NF catalyst was obtained.

Preparation of Mo-NiS@NF, NiVS@NF and NiS@NF

For comparison, Mo-NiS@NF, NiVS@NF and NiS@NF were synthesized using the similar method. Compared with the method of Mo-NiVS@NF, Mo-NiS@NF was prepared through the above method without $Na_3VO_4 \cdot H_2O$. In turn, NiVS@NF and NiS@NF were also prepared.

Characterizations

The powder X-ray diffraction (PXRD) patterns were measured on X'Pert Pro MRDDY2094 with Cu-Kα radiation (λ = 1.5418 Å). Scanning electron microscopy (SEM) results were characterized by the SU8010. Transmission electron microscopy (TEM), high-resolution HR-TEM and EDX elemental mapping images were recorded on Talos F200x (Thermo Fischer). X-ray photoelectron spectroscopy (XPS) spectra were carried out on a Thermo Scientific K-Alpha. Raman spectrometer (XploRA, excitation wavelength of 532 nm)

Electrochemical measurements

All electrochemical experiments were performed on CHI660E electrochemical workstation with 1 M KOH aqueous solution as electrolyte. The oxygen evolution reaction (OER) performances were measured with a three-electrode system, in which as-prepared samples were employed as the working electrode, platinum plate as the counter electrode and Hg/HgO as reference electrode. The test potentials were corrected with the equation $E_{vs.\ RHE} = E_{vs.\ SCE} + 0.059pH + 0.099V$. The cyclic voltammetry (CV) test was measured from 0 V to 0.8 V with a scan rate of 5 mV s^{-1}. The reversible potentials for OER are 1.23 V *vs.* standard hydrogen electrode (SHE). Hence, the equations $\eta_{OER} = E_{RHE} - 1.23$ V can be used for OER to calculate the overpotentials at a desired current density. Tafel plots were obtained from CV curves by using the equation: $\eta = b\log(j) + a$, where η is overpotential, j is the current density, b is the Tafel slope. Double-layer capacitance values were calculated based on cyclic voltammetry (CV) curves at scan rate from 10 to 100 mV s^{-1} under the potential from 0.1 V to 0.3 V. Electrochemical impedance spectroscopy (EIS) measurements were carried out according to a certain potential with the frequency of 10^6 Hz ~ 1 KHz. In multi-current process testing, the current density increases from 20 mA·cm^{-2} to 240 mA·cm^{-2} and remains steady for each period of 500 s. Durability was performed by chronopotentiometry at a 10 mA cm^{-2} constant current.

TOF calculations

TOF can be calculated by using the electrochemistry method.[1,2] A linear relationship between the oxidation current densities for redox species and the scan rates can be obtained from the cyclic voltammograms of Mo-NiVS@NF. The quantity of the active sites (m) is calculated by the formula: slope = $n^2F^2m/4RT$, where n represents the amount of electron transfer denoted as 1, F is the Faradaic constant (96485 C mol^{-1}), *R* is the ideal gas constant (8.314 J mol^{-1} k^{-1}) and T is the absolute temperature (298 K). The TOF is calculated by the following equation: TOF = jA/4Fm, where J is the current density; A is the geometrical electrode area of the electrode, and 4 indicates the moles of electron consumption for one mole oxygen evolution.

Determination of Faradaic efficiency

The Faradaic efficiency of a catalyst in OER is defined as the ratio of the amount of O_2 evolved during the experiments to the amount of the theoretical O_2 yield.[3,4] The actual O_2 output was obtained by water drainage method. The system was then tested under a current density of 50 mA cm^{-2} for 3600 s. And then calculated the moles of O_2 generated from the reaction with an ideal gas law: pV = nRT, where p is the pressure, V is the gas volume, T is the temperature, n is the amount of substance, and R is the ideal gas constant. As for the theoretical value, we assumed that 100% current efficiency occurs during the reaction, which means only the OER process takes place at the working electrode. We can then calculate the theoretical amount of O_2 evolved by applying the Faraday law: Faraday efficiency= mnF / It, where m is the mole number of the O_2, n is the number of reaction electrons, F is the Faraday constant, I is the current, and t is the time.

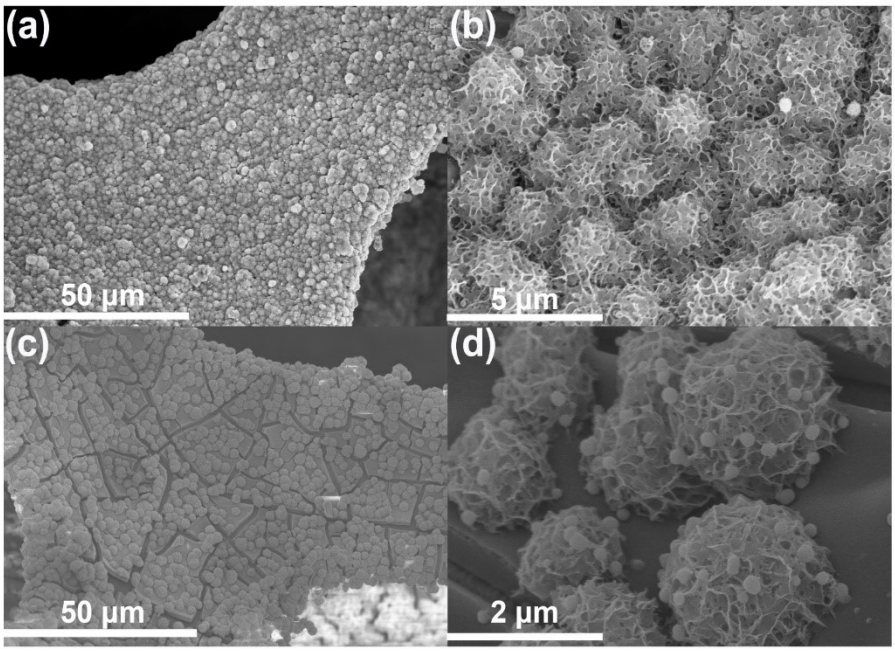

Fig. S1 SEM images of Ni-BTC@NF(a) and (b), Mo-Ni-BTC@NF (c) and (d).

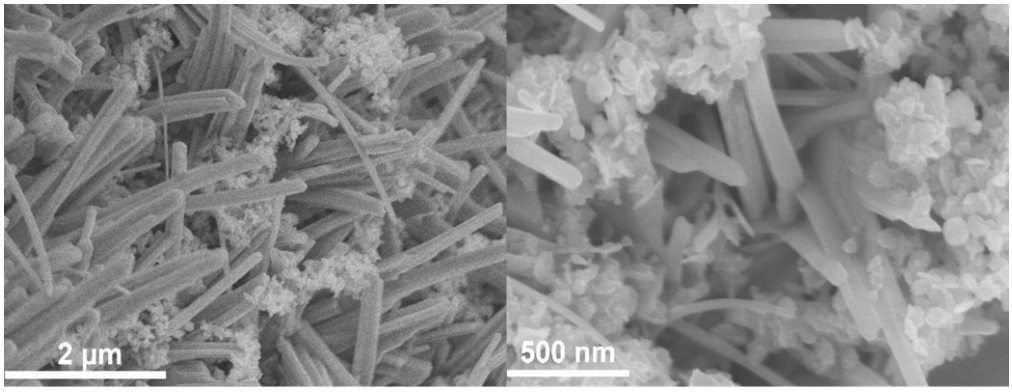

Fig. S2 SEM images of Mo-NiVS@NF.

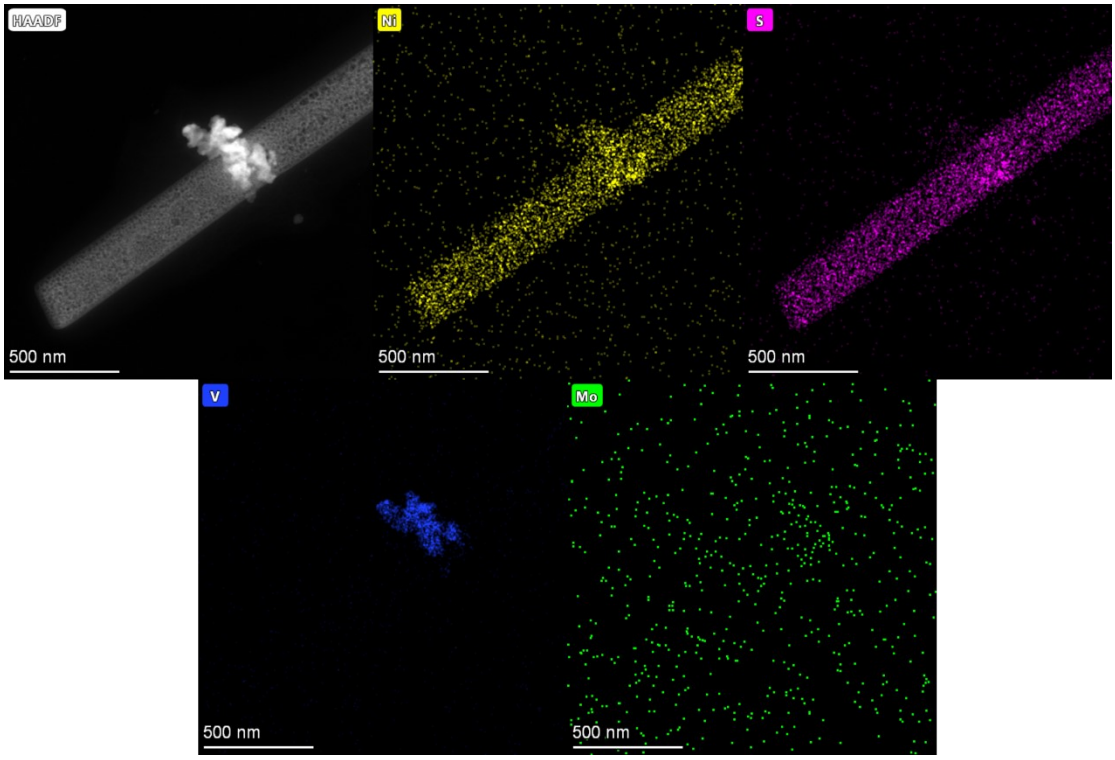

Fig. S3 EDS elemental mapping images of Ni, S, V and Mo in Mo-NiVS@NF.

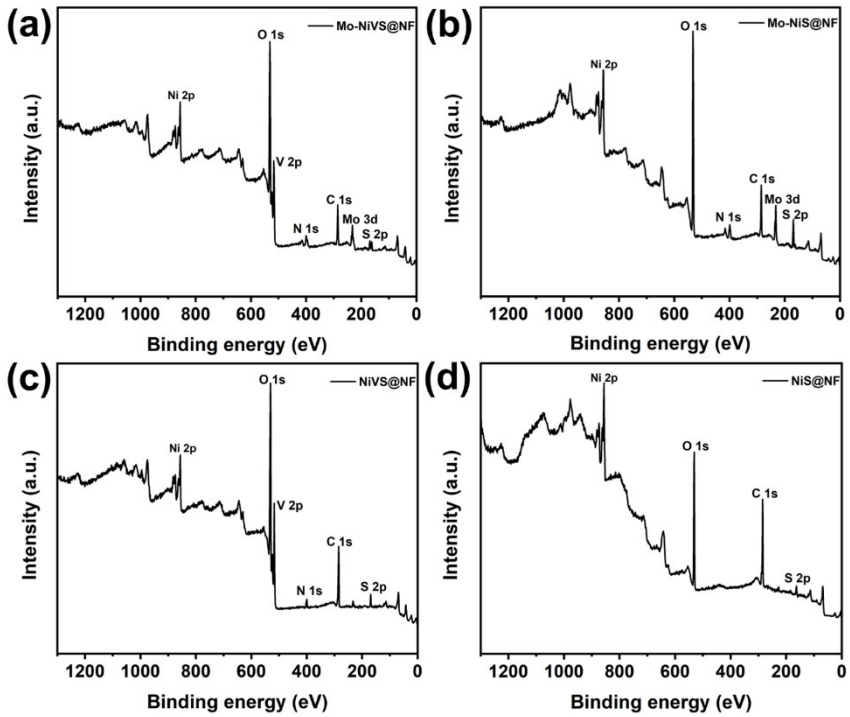

Fig. S4 The survey XPS spectra of Mo-NiVS@NF (a), Mo-NiS@NF (b), NiVS@NF(c) and NiS@NF(d).

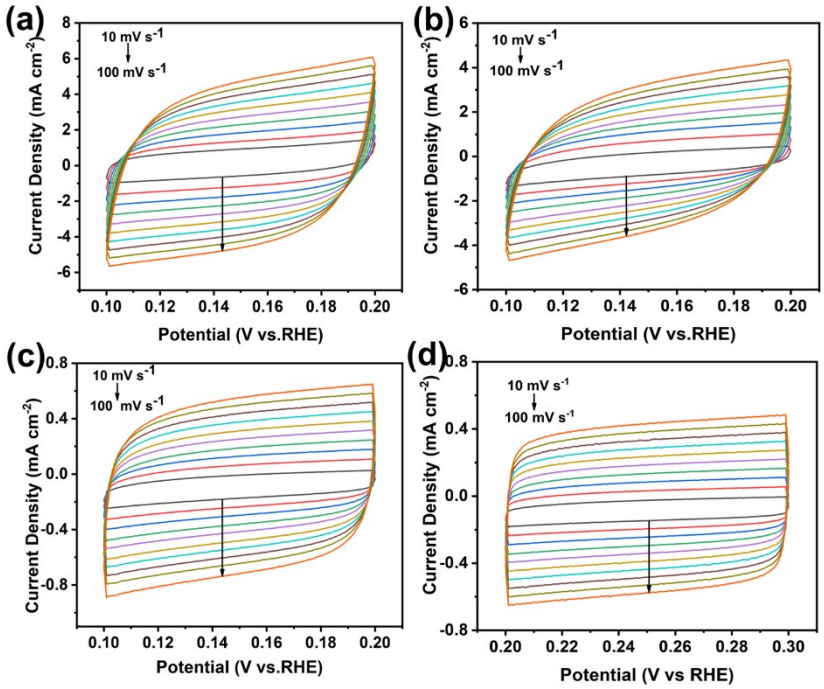

Fig. S5 CVs of Mo-NiVS@NF (a), NiVS@NF (b), Mo-NiS@NF (c) and NiS@NF (d) at the scan rate range from 10 to 100 mV·s^{-1}.

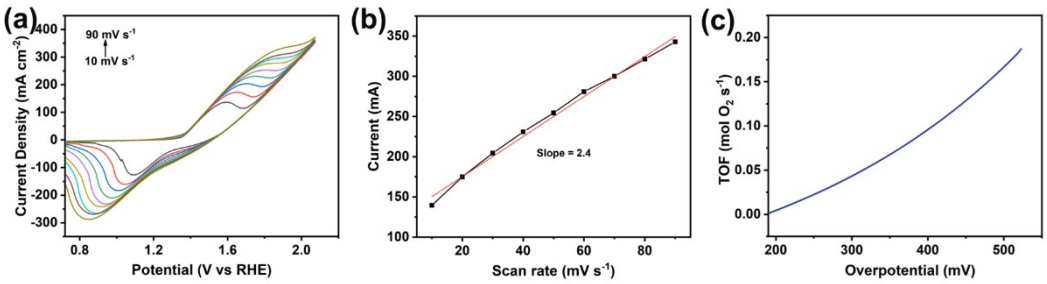

Fig. S6 (a) CVs of Mo-NiVS@NF with different scan rates increasing from 10 to 90 mV s^{-1}, (b) a linear plot between the oxidation currents and scan rates and (c) plot of the TOF of Mo-NiVS@NF as a function of the overpotential.

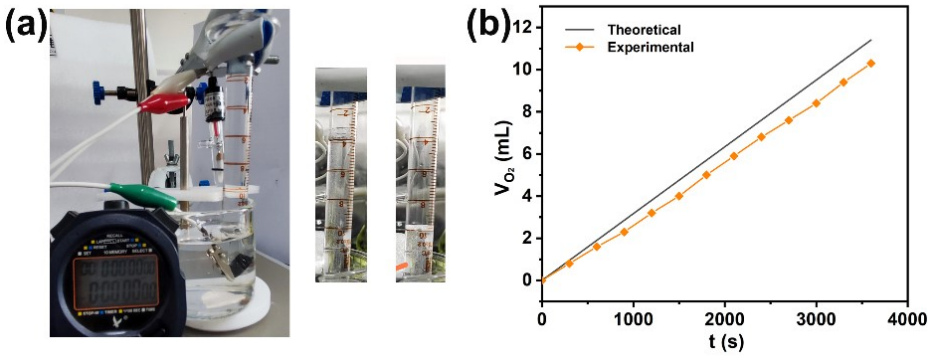

Fig. S7 (a) Experimental device, and (b) theoretical and experimental data of the Faradaic efficiency at 50 mA in 1 M KOH of Mo-NiVS@NF.

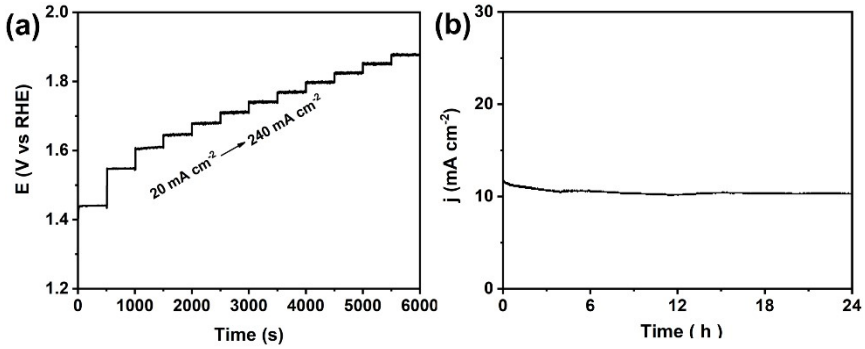

Fig. S8 (a) Multi-current process of Mo-NiVS@NF for OER in 1 M KOH ranging from 20 mA cm^{-2} to 240 mA cm^{-2}, (b) Chronopotentiometric curve at 10 mA cm^{-2} over 24 h for Mo-NiVS@NF.

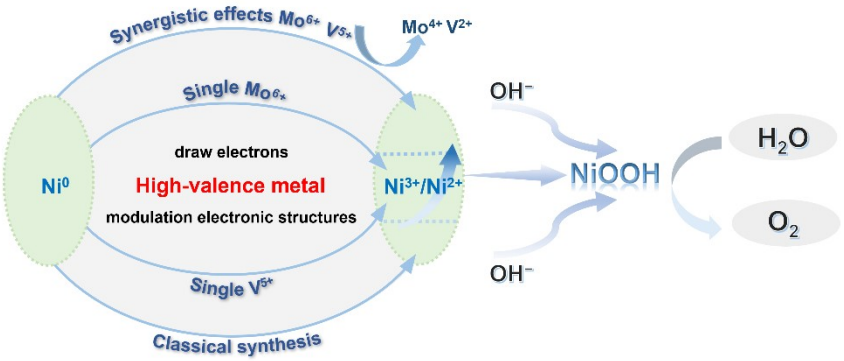

Fig. S9 The mechanism of as-obtained Mo-NiVS@NF for OER.

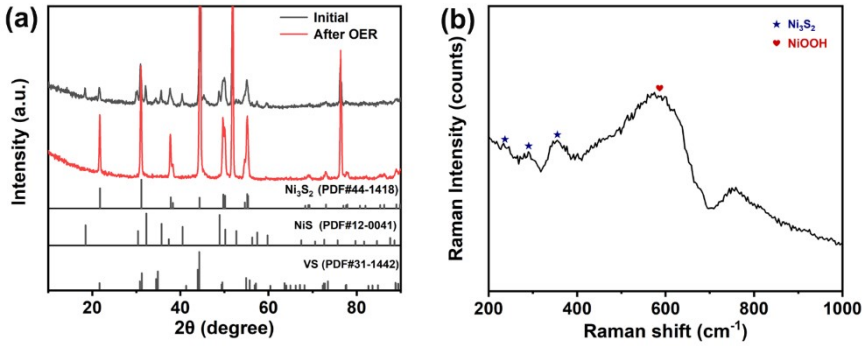

Fig. S10 (a) XRD patterns and (b) Raman spectra of the Mo-NiVS@NF after OER stability test.

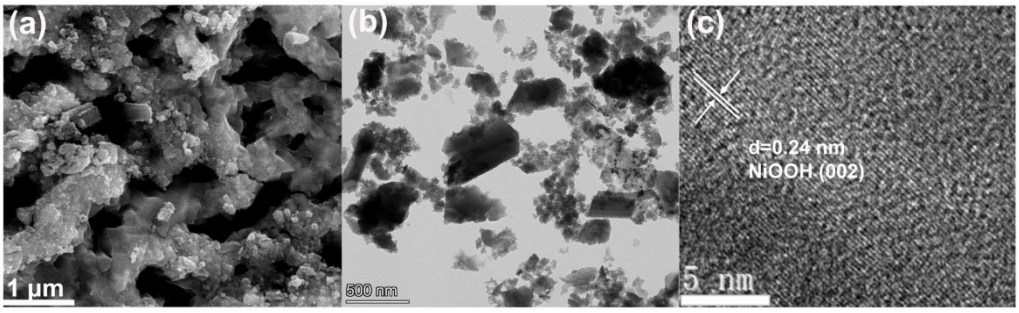

Fig. S11 (a) SEM, (b) TEM and (c) HRTEM images of Mo-NiVS@NF after OER stability test.

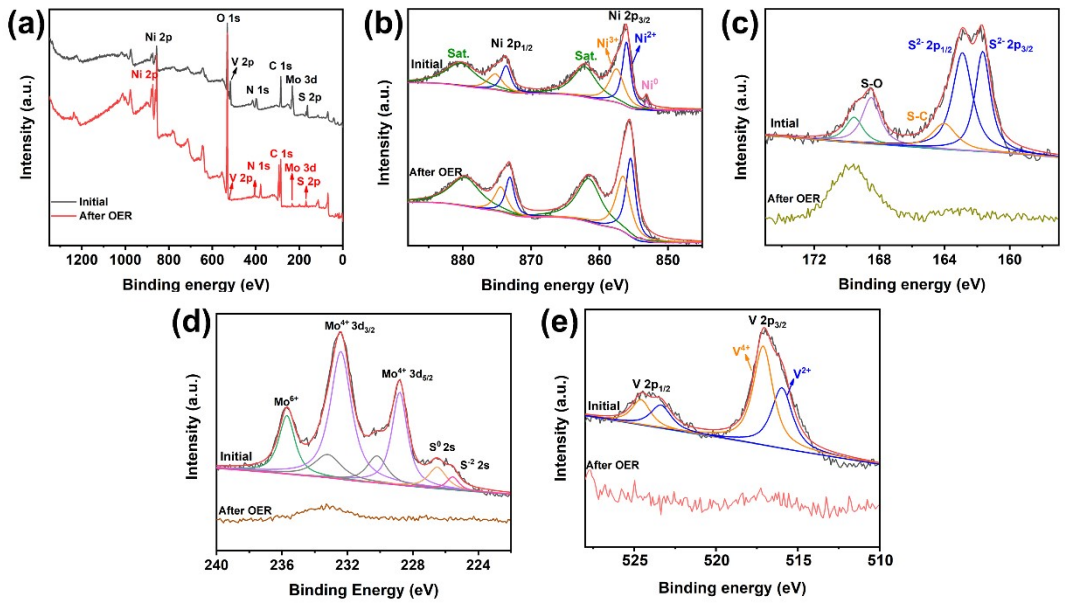

Fig. S12 The survey XPS spectra (a), high-resolution XPS spectra of Mo-NiVS@NF before and after OER stability test (b-e).

Table S1. Comparison of OER performance for Mo-NiVS@NF with other NiS-based electrocatalysts in 1 M KOH solution.

Catalyst	Current density (mA cm^{-2})	Overpotential (mV vs RHE)	Tafel slope (mV dec^{-1})	Reference
Mo-NiVS@NF	**10**	**217**	**53.6**	**This work**
F-Ni_3S_2	10	239	36	5
Ni_3S_2/MoS_2	10	260	68	6
NiS/VS	10	240	71.2	7
Ni_3S_2@$FeNi_2S_4$@NF	10	235	92	8
FCC-Ni-NiS/NS-rGO	10	254	112	9
MnCo@NiS	10	286	31.5	10
Co_3O_4@Ni_3S_2/NF	20	260	121.7	11
Ni_3S_2-Co_9S_8	20	294	80	12
Ni_3S_2@FeNi-$NiFe_2O_4$/C	10	280	33.9	13
Ni-Ni_3S_2	10	284.7	56	14
Ni_3S_2@C@CNS	10	298	51.3	15
Fe- Ni_3S_2/FeNi	10	282	54	16
BG@Ni/Ni_3S_2	10	320	41	17
Fe-doped Ni_3S_2	10	295	71	18
NF-Ni_3S_2/MnO_2	10	260	61	19

References

1. X. Luan, H. Du, Y. Kong, F. Qu and L. Lu, *Chem. Commun*., 2019, **55**, 7335-7338.
2. M. Xie, Y. Ma, D. Lin, C. Xu, F. Xie and W. Zeng, *Nanoscale*, 2020, **12**, 67-71.
3. T. Gao, C. Zhou, Y. Zhang, Z. Jin, H. Yuan and D. Xiao, *J. Mater. Chem. A*, 2018, **6**, 21577-21584.
4. J. Kibsgaard and T. F. Jaramillo, Angew. *Chem. Int. Ed. Engl.*, 2014, **53**, 14433-7.
5. Q. Xu, M. Chu, M. Liu, J. Zhang, H. Jiang and C. Li, *Chem. Eng. J*., 2021, **411**, 128488.
6. C. Wang, X. Shao, J. Pan, J. Hu and X. Xu, *Appl. Catal. B: Environ*., 2020, **268**, 118435.
7. K. Bao, Y. Yan, T. Liu, T. Xu, J. Cao and J. Qi, *Inorg. Chem. Front.*, 2020, **7**, 4924-4929.
8. Y. Yang, H. Meng, C. Kong, S. Yan, W. Ma, H. Zhu, F. Ma, C. Wang and Z. Hu, *J. Colloid Interface Sci*., 2021, **599**, 300-312.
9. M. B. Zakaria, Y. Guo, J. Na, R. Tahawy, T. Chikyow, W. A. El-Said, D. A. El-Hady, W. Alshitari, Y. Yamauchi and J. Lin, *ChemSusChem*, 2020, **13**, 3269-3276.
10. X. Wang, L. Li, L. Xu, Z. Wang, Z. Wu, Z. Liu and P. Yangs, *J. Power Sources*, 2021, **489**, 229525.
11. Y. Gong, Z. Xu, H. Pan, Y. Lin, Z. Yang and X. Du, *J. Mater. Chem. A*, 2018, **6**, 5098-5106.
12. R. Zhang, L. Cheng, Z. Wang, F. Kong, Y. Tsegazab, W. Lv and W. Wang, *Appl. Surf. Sci*., 2020, **526**, 146753.
13. L. Xu, S. Ali Shah, H. Khan, R. Sayyar, X. Shen, I. Khan, A. Yuan, W. Yaseen, Z. Ali Ghazi, A. Naeem, H. Ullah, X. Li and C. Wang, *J. Colloid Interface Sci*., 2022, **617**, 1-10.
14. Y. Lin, G. Chen, H. Wan, F. Chen, X. Liu and R. Ma, *Small*, 2019, **15**, 1900348.
15. M. Al-Mamun, H. Yin, P. Liu, X. Su, H. Zhang, H. Yang, D. Wang, Z. Tang, Y. Wang and H. Zhao, *Nano Res*., 2017, **10**, 3522-3533.
16. C. Z. Yuan, Z. T. Sun, Y. F. Jiang, Z. K. Yang, N. Jiang, Z. W. Zhao, U. Y. Qazi, W. H. Zhang and A. W. Xu, *Small*, 2017, **13**, 1604161.
17. K. Zhang, X. Min, T. Zhang, M. Si, J. Jiang, L. Chai and Y. Shi, *ACS Appl. Mater. Interfaces*, 2020, **12**, 54553-54562.
18. Y. Zhu, H. Yang, K. Lan, K. Iqbal, Y. Liu, P. Ma, Z. Zhao, S. Luo, Y. Luo and J. Ma, *Nanoscale*, 2019, **11**, 2355-2365.
19. Y. Xiong, L. Xu, C. Jin and Q. Sun, *Appl. Catal. B: Environ*., 2019, **254**, 329-338.